Level-crossing downsampling for quantization error reduction in sine wave estimation

D.J. De Beer, *Member, IEEE*, and T-H. Joubert, *Senior Member, IEEE*

***Abstract*—This work introduces a digital post-processing algorithm—level-crossing downsampling (LC-DS)—for estimating sine-wave parameters from sequences of quantized values acquired by standard ADCs. LC-DS emulates level-crossing sampling by retaining only transition points, reducing correlated quantization error and accelerating least-squares regression. Its performance is benchmarked against uniform least-squares regression and calibrated sinefit to highlight accuracy and computational trade-offs. Across a wide dynamic range, LC-DS consistently outperforms uniform sampling and approaches the accuracy of calibrated sinefit for low-level signals, while remaining up to two orders of magnitude faster for large datasets. Unlike conventional methods, LC-DS scales efficiently with data size, enabling real-time estimation without hardware modifications. Practical and simulated experiments, including electrochemical impedance spectroscopy, confirm robustness under conditions such as signal saturation. These results position LC-DS as a compelling alternative for applications requiring both high precision and computational efficiency.**

***Index Terms*—real-time signal processing, sine wave estimation, quantization, least squares regression, electrochemical impedance spectroscopy**

I. Introduction

Many sensor applications rely on accurately measuring the parameters of a sine wave. These applications include three-dimensional (3D) mapping [1, 2], device testing [3, 4], light detection and ranging (LiDAR) [5], localization [6], vibration control [7], frequency estimation [8], organ analysis [9, 10], rotational speed measurements [11], Planck-balance measurement [12], and electrochemical impedance spectroscopy (EIS) [13–17]. This work primarily develops for EIS, and therefore, its results are discussed within the context of EIS. Standard EIS systems typically construct an impedance spectrum by discretely stepping through a range of single frequencies, measuring the impedance at each step individually. This makes EIS particularly useful for quantifying the performance of single sine wave estimation approaches due to the large dynamic range and wide frequency ranges of the estimated sine waves. Consequently, performance observed in specific EIS examples can be extrapolated to other applications sharing similar signal sizes and frequencies.

To estimate these parameters, the analog signal must first be captured digitally. This is achieved through an analog-to-digital converter (ADC) that converts the analog signal to a digital representation, which can then be manipulated by digital signal processing systems [18]. The most common family of ADCs is reference-based ADCs, where the digital output is latched to the nearest ADC reference level each time the ADC is clocked [19]. Quantization error is inherent to this process. This type of noise results from the finite resolution of the ADC, which can only represent the signal with a limited number of discrete levels [20, 21]. For a sine wave, a portion of the quantization error can become correlated with the signal, preventing it from averaging to zero regardless of the number of samples [22]. This leads to errors in parameter estimation, which is critical in precision applications such as EIS.

Once the signal is digitized, the challenge lies in accurately extracting the sine wave parameters despite this error. Sine wave estimation is broadly categorized into three-parameter (amplitude, phase, offset) and four-parameter estimation (adding frequency) [23]. While three-parameter estimation offers closed-form linear solutions for computational speed, four-parameter estimation is often preferred, even when frequency is nominally known, to account for potential mismatches between the apparent and true signal frequency [4, 23]. However, standard algorithmic approaches struggle to handle correlated quantization noise. The discrete Fourier transform (DFT) is the most commonly employed method for sine wave parameter estimation, but this method can have estimation errors due to spectral leakage. A more robust alternative is least squares regression (LSR) [22–24], but it does not inherently remove correlated quantization error.

To overcome these limitations, more recent work has introduced calibration-based estimators which can achieve near noise-floor accuracy. Most notably, the calibrated sinefit method [25, 26] uses a special cost function, along with computationally intensive iterative optimization. An alternative hardware-based approach, the level-crossing ADC (LC-ADC), has also shown promise but faces limitations in complexity and implementation cost. This leaves a critical gap for a method that can eliminate quantization error without needing calibration or specialized hardware.

This paper introduces a digital post-processing algorithm—level-crossing downsampling (LC-DS)—that fills this gap by emulating level-crossing sampling using data from reference-based ADCs. By algorithmically retaining only the points where the signal transitions between ADC levels, LC-DS simultaneously reduces correlated quantization error and accelerates the computation of the least-squares regression. The performance of LC-DS is benchmarked against both the traditional uniform LSR and the state-of-the-art calibrated sinefit method [25]. Physical measurements demonstrate the real-world functionality of the LC-DS method and simulations are used to explore a wider sample space. The results demonstrate

D.J. De Beer is with the Department of Electrical, Electronic and Computer Engineering at the University of Pretoria, Gauteng, South Africa (e-mail: dirk.debeer@tuks.co.za).

T-H. Joubert is with the Department of Electrical, Electronic and Computer Engineering at the University of Pretoria, Gauteng, South Africa (e-mail: trudi.joubert@up.ac.za)

that LC-DS approaches near noise-floor accuracy for small signals while being up to two orders of magnitude faster for large datasets, establishing it as a compelling choice for real-time applications.

II. Fundamentals of Sine Wave Measurement and Sampling

A sine wave is fully described by

$$A\sin(2\pi ft+\theta)+C, \tag{1}$$

where t is time and the other four variables are the parameters of a sine wave, namely amplitude (A), frequency (f), phase (θ), and constant offset (C).

A. Sine Wave Parameter Estimation Algorithms

Once a sine wave has been digitized, its parameters can be estimated using various algorithms. Spectral analysis via the DFT is the standard approach, while LSR serves as a common parametric alternative that relaxes synchronization requirements [22]. For achieving the highest accuracy, calibration-based estimators, such as the calibrated sinefit method [25, 26], have been introduced. This paper benchmarks the proposed method against uniform sampling with DFT/LSR, representing the standard robust approach, and calibrated sinefit, representing the state-of-the-art in accuracy.

1) Discrete Fourier Transform (DFT): The DFT is the most established method for spectral analysis and is commonly used in EIS to extract the amplitude and phase of the response signal. It operates by correlating the input signal with reference sine and cosine waves at fixed frequency bins.

If the signal frequency is not perfectly synchronized with one of these fixed bins, the DFT suffers from spectral leakage, where signal energy disperses into adjacent frequency bins, degrading accuracy. This can be mitigated by applying windowing functions at the cost of additional computational complexity [27].

2) Least-Squares Regression (LSR): LSR fits a sinusoidal model to sampled data by minimizing the sum of squared differences between observed and predicted values. Unlike the DFT, sampled data can be modeled using sine waves of arbitrary frequency; thus, LSR does not require coherent sampling (where the signal frequency is perfectly periodic over the sample record). Notably, in the coherent case, LSR and the DFT yield identical estimates [4]. A distinct advantage of LSR is its immunity to spectral leakage, rendering it superior to the DFT in many applications [24, 28].

Computationally, four-parameter LSR requires iterative methods, which can be slow. Conversely, if the frequency is known, the three-parameter problem becomes linear, allowing a closed-form solution that significantly improves computational efficiency. The closed-form three-parameter LSR solution remains attractive for real-time applications when frequency is known, but its accuracy is fundamentally limited by quantization artifacts in uniform sampling. This motivates alternative strategies that either modify the estimator (e.g., calibrated sinefit) or modify the data itself (e.g., the LC-DS approach proposed in this paper).

To derive the closed-form solution, we can rewrite (1) in a linear form. Using the trigonometric sum identity, we can express the sine wave as:

$$Q\sin(2\pi ft)+I\cos(2\pi ft)+C. \tag{2}$$

The relation between Q and I and the original amplitude and phase is given by $A=\sqrt{Q^2+I^2}$ and $\theta=\arctan\left(\frac{I}{Q}\right)$. This transformation makes the problem linear with respect to the parameters Q, I, and C.

Given N sampled data points (t_k, y_k), one can construct a linear system

$$\mathbf{y}=\mathbf{X}\boldsymbol{\beta}+\boldsymbol{\epsilon}, \tag{3}$$

where:

- $\mathbf{y}$ is the observation vector $\begin{bmatrix}y_1 & \dots & y_N\end{bmatrix}^T$,
- $\boldsymbol{\beta}$ is the parameter vector $\begin{bmatrix}Q & I & C\end{bmatrix}^T$ that is estimated,
- $\mathbf{X}$ is the $N\times 3$ design matrix with rows of the form $\begin{bmatrix}\sin(2\pi ft_k) & \cos(2\pi ft_k) & 1\end{bmatrix}$, and
- $\boldsymbol{\epsilon}$ is the residual error vector.

The least squares solution for $\boldsymbol{\beta}$ minimizes the sum of squared errors. The closed-form solution is then:

$$\boldsymbol{\beta}=(\mathbf{X}^T\mathbf{X})^{-1}\mathbf{X}^T\mathbf{y} \tag{4}$$

This allows a direct calculation of Q, I, and C from the sampled data, provided the matrix $(\mathbf{X}^T\mathbf{X})$ is invertible.

3) Calibrated Sinefit: The calibrated sinefit method achieves near noise-floor accuracy by directly addressing quantization error [25]. Unlike classical methods that operate on the quantized output values, this technique uses knowledge of the ADC's transition levels. These levels can be determined beforehand through a precise calibration procedure or simply assumed to be ideal for a given ADC resolution. The algorithm then iteratively adjusts the sine wave parameters (A, θ, C) to find the curve that best fits the observed sequence of ADC output codes, consistent with the known or assumed transition levels. While this method can effectively eliminate quantization bias and approaches the noise floor, its computationally intensive iterative optimization still limits its use in real-time or low-cost systems where such overhead is impractical.

B. Sampling Considerations for Accurate Measurement

The process of analog-to-digital conversion and the characteristics of the sampled data profoundly impact the accuracy and reliability of subsequent sine wave parameter estimation. Key considerations include the record length, N, the ratio between the signal frequency, f_i, and the sampling frequency, f_s, and the inherent noise introduced during sampling.

IEEE Std 1241-2010 [4] provides guidelines for ADC testing that are also applicable to optimizing sampling for accurate sine wave estimation [29]. It recommends choosing f_i such that N uniformly distributed phases are sampled, typically by setting

$$f_i=\left(\frac{J}{N}\right)f_s, \tag{5}$$

where J is an integer that is relatively prime to N (i.e., their greatest common divisor is one). This approach ensures

coherent sampling, where exactly J cycles of the sine wave are captured within the record N, which helps minimize spectral leakage and improve estimation accuracy.

1) Quantization Error as a Sampling Artifact: Quantization error is treated here as a dominant source of estimation bias, rather than as an ADC performance metric. Unlike uniform sampling, LC-DS reduces this bias by converting time-based samples into amplitude-based transition points, which decorrelates quantization error from the signal. This section sets the stage for comparing LC-DS against uniform sampling with DFT, LSR, and calibrated sinefit in terms of accuracy and computational efficiency.

Quantization error is an unavoidable artifact introduced during the analog-to-digital conversion process, arising from the finite resolution of the ADC that maps continuous analog signals to discrete digital values [20, 21]. The impact and characteristics of this error within the sampled data depend significantly on the sampling conditions, particularly whether the sampling is coherent or incoherent.

In coherent sampling, where the data record contains an integer number of sine wave cycles, the periodicity of the signal within the observation window helps to distribute the quantization error more uniformly across the frequency spectrum. If the number of cycles, J, is co-prime with the record length, N, this minimizes impact of quantization error on estimated parameters [4]. Conversely, if J and N share common factors, the effective number of unique samples is reduced. Therefore, coherent sampling does not necessarily lead to N unique samples over a record length of N, which can compound quantization error and lead to less accurate estimates. When implemented correctly, coherent sampling enables more accurate parameter estimation due to the alignment of the signal period with discrete sampling intervals, reducing aliasing and spectral leakage.

In contrast, incoherent sampling occurs when the data record does not contain an integer number of sine wave cycles. This lack of periodicity leads to spectral leakage, where the signal's energy spreads into adjacent frequency bins, complicating the estimation process. While the non-uniform distribution of quantization error in incoherent sampling can sometimes yield better sine wave estimates than non-co-prime coherent sampling, it generally results in less accurate parameter estimates compared to properly executed co-prime coherent sampling.

In practical EIS systems, where the signal source and sampling subsystem are tied to the same master clock, coherent sampling can easily be forced. However, the signal source (typically a direct digital synthesizer) has a much finer frequency resolution than a typical low-cost ADC. Enforcing strict coherence can therefore result in only a subset of all direct digital synthesizer frequencies being used. Accurate estimation in incoherent cases can therefore enable higher frequency resolution in low-cost systems.

Ultimately, quantization error will always be present in sampled data when the combination of a sine wave amplitude, offset, and phase does not align precisely such that all quantization error averages to zero. While a theoretical case exists where ideal parameters could lead to zero quantization error, this is rare in practice. In typical applications, such perfect alignment is absent, leading to significant quantization error manifesting in the measurement, which can adversely affect the accuracy of sine wave parameter estimation. Addressing this sampling-induced quantization error is therefore critical for improving measurement accuracy [22].

III. Proposed Level-crossing Downsampling Processing

While hardware-level solutions such as level-crossing ADCs exist [19, 30], they require specialized hardware and complex reconstruction. The proposed level-crossing downsampling (LC-DS) algorithm emulates these benefits in software using uniformly sampled data, enabling similar accuracy improvements without hardware changes or calibration. LC-DS is founded on the principle of algorithmically transforming digital data acquired from a reference-based ADC, making it suitable for low-cost and real-time applications. This technique effectively re-frames the challenge of correlated quantization error, which is a consequence of the finite resolution of discrete reference levels, into an issue of temporal accuracy. This approach reduces estimation bias and accelerates least-squares regression without requiring prior calibration or iterative optimization.

The initial step of this process involves acquiring digital signal data from a reference-based ADC. An output is subsequently generated at each instance where two adjacent ADC samples differ. To preserve the essential time and frequency information required for accurate sine wave parameter estimation, the precise time (or sample index) at which this change occurred must also be captured. The procedure is outlined below.

Let the input sequence of uniformly sampled ADC data be denoted as y, with length N, and its elements as y_i for $i \in \{0, 1, \ldots, N-1\}$. The corresponding sequence of sample times is t, with elements t_i.

$$y = \{y_0, y_1, \ldots, y_{N-1}\} \tag{6}$$

$$t = \{t_0, t_1, \ldots, t_{N-1}\} \tag{7}$$

When the analog input signal transitions between two adjacent ADC quantization levels, say from y_{i-1} to y_i (where the values are not equal), the proposed method generates a new downsampled data point. This new point is assigned the midpoint value between the two sampled ADC levels.

The critical aspect of this method lies in the accuracy of the amplitude assigned to this midpoint value. Based on the intermediate value theorem (IVT), if a continuous function (like a sine wave) takes on two values y_{i-1} and y_i at times t_{i-1} and t_i, respectively, then it must take on every value between y_{i-1} and y_i at some time between t_{i-1} and t_i [31].

Crucially, for a sufficiently high sampling rate, the segment of the sine wave between two consecutive samples can be approximated as linear. Under this linear assumption, the true analog signal value at the effective midpoint time between t_{i-1} and t_i is very closely approximated by the midpoint amplitude. This selection of the midpoint amplitude, rather than either of the quantized levels, significantly enhances the accuracy of the sampled amplitude point while reducing the number of points.

The time associated with this midpoint value is assigned as the midpoint of the original sample times. This leads to a new sequence of times, t', that consists of subsamples of t but shifted by an index offset of -0.5. While the precise alignment of the output index by half a step (e.g., $i-0.5$ for unit-spaced indices) reflects the interpolated nature of this new data point, this exact time shift is not strictly algorithmically necessary for the core downsampling function.

This procedure generates new amplitude and time data points for each instance where the input signal transitions between ADC levels. For the k-th such transition occurring between original sample indices $i-1$ and i, the new amplitude and time points are defined as:

$$y'_k = \frac{y_i + y_{i-1}}{2}, \quad \text{and} \tag{8}$$

$$t'_k = \frac{t_i + t_{i-1}}{2}. \tag{9}$$

This applies for all $i \in \{1, \ldots, N-1\}$ where $y_i \neq y_{i-1}$.

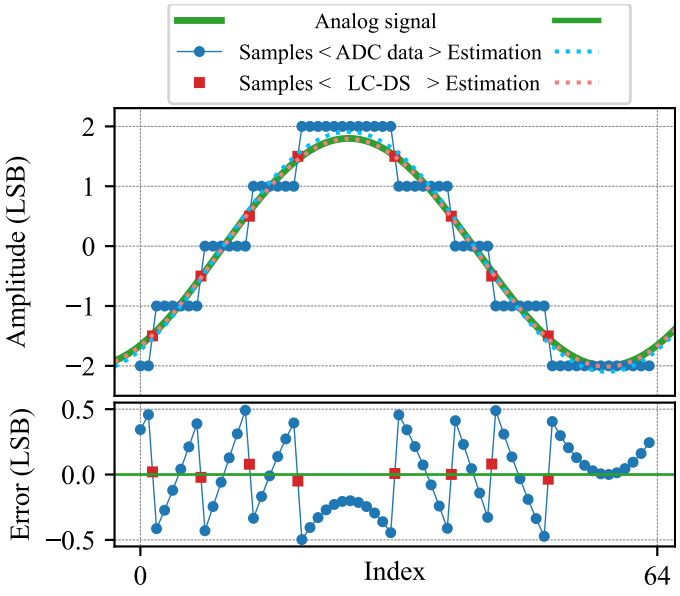

Fig. 1. Input and output of the LC-DS procedure as well as the resultant quantization error over 64 samples of a coherently sampled sine wave.

The LC-DS process is illustrated in Fig. 1, showing how level-crossing downsampling transforms uniformly sampled data into transition-based samples and reduces quantization error. For uniform sampling, the quantization error of samples immediately before and after a level transition tends toward ± 0.5 LSB, corresponding to the threshold edges. As the sampling rate increases, these two points become arbitrarily close in time, while each error approaches its respective threshold edge. Consequently, the midpoint between them converges to the true signal value, effectively driving the estimation error toward zero.

One can see from Fig. 1 that while the quantization error is approximately linear around the sine wave edges, that is not the case at the sine wave peak and trough. This leads to a disproportionate amount of quantization error introduced in this region of the data, that is correlated to the signal and does not average to 0. The reduction in quantization error obtained with the LC-DS technique, particularly through the precise assignment of mid-level crossing times, is also visible.

Fig. 1 additionally shows how the quantization error manifests as an amplitude estimation error. In this small example, the estimated sine wave amplitude using LC-DS is 0.13% while the error without this method is significantly larger at 5.54%. When the number of samples is increased from 64 to 512, the LC-DS estimate error improves to 0.02% while the error without LC-DS becomes 5.30%.

Beyond the reduction in quantization error due to the nature of the sampled points, the proposed method has additional benefits. For slowly changing signals, such as a sine wave that has been oversampled (or one that has been undersampled such that it has a low apparent frequency [14]), LC-DS will significantly reduce the number of samples in the dataset without compromising the estimation accuracy. This will, in turn, reduce the computational resources required to calculate the LSR for sine wave parameter estimation.

Another important benefit of the LC-DS technique is its innate ability to deal with ADC saturation. Saturation occurs when the input signal amplitude into the ADC exceeds the limits of the ADC. For such signals, the ADC will report a maximum or minimum digital value depending on whether the signal is saturating at the high or the low end of the range. The entire saturated segment of the signal will be removed by the downsampling algorithm and only the last change before saturation, and the first change thereafter, will be preserved. It was shown in [14] that saturation can improve the dynamic range of ADCs for sine wave measurements. Thus, the LC-DS algorithm enables this benefit without additional processing to detect or remove saturation from a signal.

IV. Results

This section benchmarks the performance of the proposed LC-DS algorithm against uniform sampling with DFT/LSR and the calibrated sinefit method. The evaluation uses a combination of noiseless simulated data to isolate the effects of quantization error and practical measurements from a low-cost impedance analyzer to validate the simulation findings under practical conditions. The parameters for the simulated investigations are detailed in Table I. When the sampled data is coherent and the DFT and LSR estimates are equivalent, only one trace is shown on the graph to represent both results.

A. Accuracy, Data Reduction, and Computational Speed

The first investigation explores how estimation accuracy is affected by the number of samples captured per period of the sine wave. As shown in Fig. 2, the error for uniform DFT/LSR approaches a limit, indicating its inability to overcome correlated quantization error even with more data. In contrast, the estimation error for both LC-DS and the calibrated sinefit method improves steadily as the number of samples increases. Calibrated sinefit consistently provides the lowest error, with LC-DS following a parallel trend approximately 20 dB higher for this signal size. Fig. 2 additionally illustrates the source of LC-DS's computational efficiency: as the sampling rate

TABLE I
MEASUREMENT PARAMETERS FOR SIMULATED DATA EXPERIMENTS.

Investigation	Fig(s)	Variable(s)	Fixed parameter(s)	Value(s)	Number of points
Error & Computation Time vs. Samples per Period	Figs. 2 and 3	Array length	—	128 to 32768	17
		—	Amplitude	55 ± 5 % of ADC range†	1
		—	Phase	0° to 360°	45*
		—	Offset	−0.5 LSB to 0.5 LSB	45*
Error vs. Signal Amplitude	Fig. 4	Amplitude	—	0.25 % to 500 % of ADC range	15
		—	Array length	4096	1
		—	Phase	0° to 360°	45*
		—	Offset	−0.5 LSB to 0.5 LSB	45*
Error vs. Phase and Offset	Fig. 5	Phase	—	0° to 360°	45
		Offset	—	−0.5 LSB to 0.5 LSB	45
		—	Array length	4096	1
		—	Amplitude	50 ± 5 % of ADC range†	1

† Randomly fixed for each run within this range to avoid bias.
* When the number of points for a fixed value is greater than 1, the average is taken over those points.

increases, the data reduction percentage approaches 100%, meaning the subsequent LSR algorithm processes only a small fraction of the original samples.

The computational efficiency of the methods was evaluated by measuring their average execution time as a function of the number of samples, with the results shown in Fig. 3. While theoretically all four methods have a computational complexity that scales linearly with the number of samples, $O(N)$, their practical performance is dictated by significantly different computational overheads.

The iterative nature of the calibrated sinefit method imposes the highest overhead, making it the most computationally intensive. The DFT is the fastest method when the number of samples is low, but its complexity scales as the number of samples increases, nearly matching the complexity of the closed-form LSR. The key advantage of LC-DS is that its most demanding computational steps scale not with the total number of samples N, but with the much smaller number of level crossings. This is a direct result of the data reduction shown in Fig. 2, which leads to a substantially lower effective time per sample. Consequently, LC-DS becomes faster than the competing methods once the number of samples exceeds approximately 2^{11}, and achieves a speed-up of more than two orders of magnitude compared to calibrated sinefit at 2^{15} samples.

For applications like EIS, performance across a wide dynamic range is critical. Fig. 4 investigates the absolute error as a function of signal amplitude. The results reveal a key characteristic of the LC-DS method. For small signals (below 10% of the ADC's range), both LC-DS and calibrated sinefit show a significant reduction in error compared to uniform DFT/LSR, with their error being over 50 dB lower. In this small-signal region, the performance of LC-DS is nearly identical to the calibrated sinefit method. As signal amplitude increases towards 100% of the ADC range, the performance of the two methods diverges, with the error of calibrated sinefit becoming approximately 20 dB lower than that of LC-DS. Furthermore, the plot extends into the ADC saturation where the error for uniform DFT/LSR increases significantly.

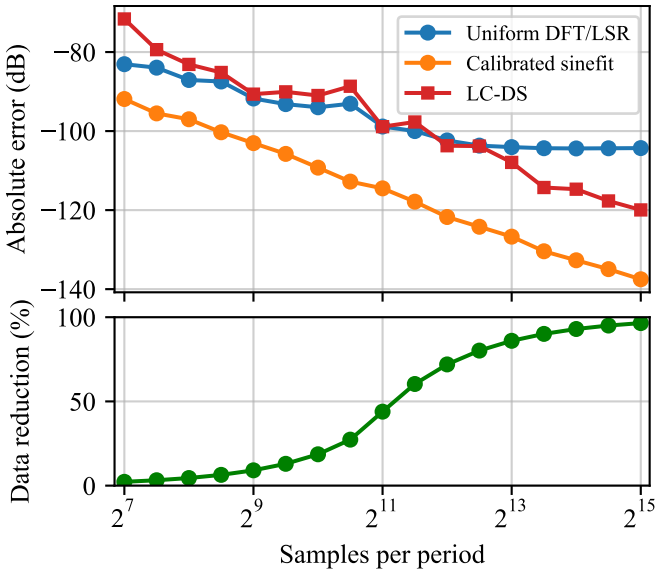

Fig. 2. Absolute error as a function of samples per period for uniform DFT/LSR, calibrated sinefit, and LC-DS. The figure additionally shows the corresponding data reduction achieved by LC-DS.

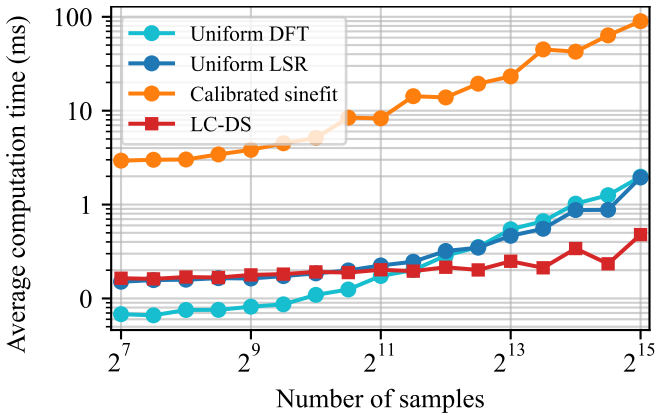

Fig. 3. Average computation time versus number of samples for the four benchmarked methods.

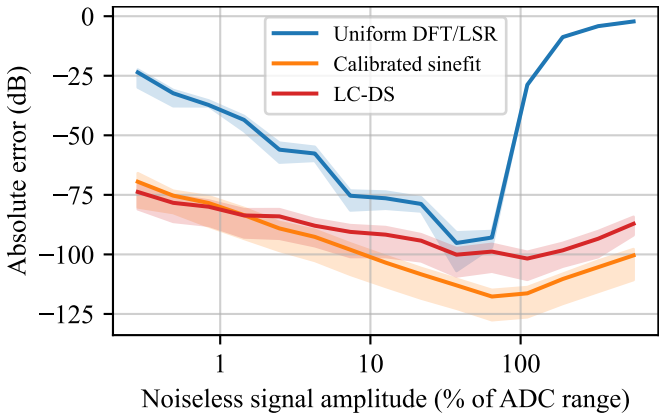

Fig. 4. Absolute error due to quantization as a function of signal size for LC-DS, calibrated sinefit, and uniform sampling DFT/LSR. The shaded region around each line indicates the interquartile range of the data.

In contrast, LC-DS and calibrated sinefit maintain low error, demonstrating their innate ability to handle saturated signals.

B. Performance Under Specific Conditions

To visualize the sensitivity of each method to small variations in signal phase and offset, Fig. 5 presents 2D heat maps of the estimation error. The plot for uniform DFT/LSR shows distinct vertical bands, confirming a strong correlation between quantization error and the signal's DC offset. In contrast, both LC-DS and calibrated sinefit exhibit much lower average error (−93 dB and −106 dB, respectively, versus −76 dB for uniform DFT/LSR) and show no strong correlation to either phase or offset. Fig. 5 also shows the computation time required to generate each dataset (runtime), where it can be seen that LC-DS required only 0.51 s whereas calibrated sinefit required 31.4 s.

C. Practical Measurement Validation

Finally, to validate the simulation results, practical measurements were performed on a physical "R-RC" impedance model using a low-cost impedance analyzer setup shown in Fig. 6 [14, 15]. The custom device uses a dsPIC33EV microcontroller's integrated ADC module for sampling. The ADC is configured to a 10-bit resolution and the sampling rate is adaptive to achieve coherent sampling. The measured "R-RC" impedance model is based on the impedance spectrum of salt dissolved in water measured using a gold interdigitated electrode and consists of a 270 Ω resistor in series with a parallel combination of a 12 kΩ resistor and 100 nF capacitor. As depicted in Fig. 6, the setup is shown during an active measurement of this "R-RC" model. The digital oscilloscope displays the raw analog signals directly from the measurement probes, while the laptop shows real-time oscillograms generated from the data acquired by the low-cost device.

The resulting Nyquist plot is shown in Fig. 7. The right side of the plot corresponds to high impedance values, which in turn produce very small current signals at the ADC input. In this small-signal region, the quantization error becomes dominant. The data points from uniform DFT/LSR show a significant spread along the magnitude lines, indicating poor precision. In contrast, the data points for both LC-DS and calibrated sinefit are tightly clustered and aligned with the fitted model, confirming their superior accuracy and precision. These practical results corroborate the key finding from the simulations: LC-DS effectively mitigates quantization error in real-world measurements, performing comparably to the state-of-the-art method for the most challenging small-signal conditions.

D. Performance Summary

The trade-offs of the three considered methods are explored in Table II. Based on this qualitative comparison, LC-DS is well positioned as a fast (real-time) estimation technique that achieves estimations accuracy between that of the typical LSR approach, and the computationally intensive calibrated sinefit method.

V. Conclusion

In this paper, the efficacy of the newly proposed LC-DS digital post-processing algorithm was explored in the

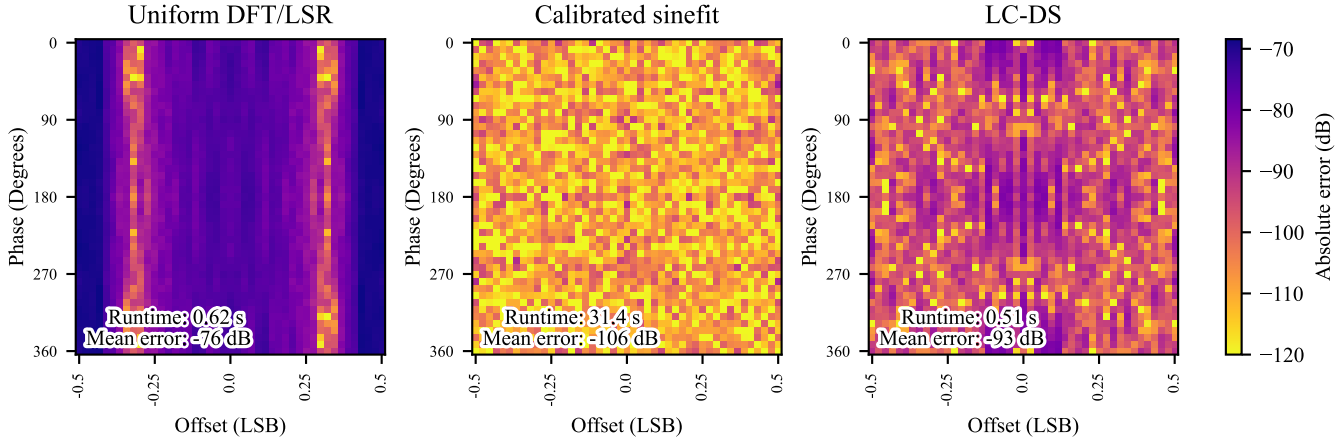

Fig. 5. Heat maps of absolute error due to quantization compared between LC-DS, uniform sampling DFT/LSR, and calibrated sinefit, showing sensitivity to initial phase and offset.

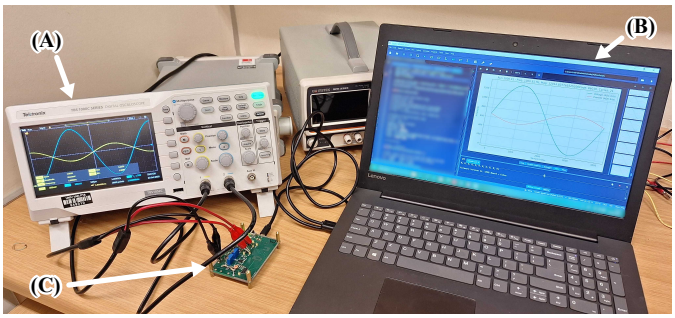

Fig. 6. The practical measurement setup. (A) Tektronix digital oscilloscope, (B) laptop computer for control and (C) a custom low-cost impedance analyzer [14, 15].

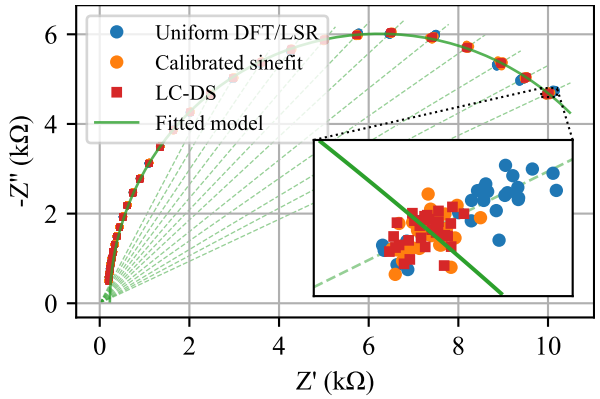

Fig. 7. Nyquist plot of an "R-RC" impedance model measured using a low-cost impedance analyzer, comparing uniform sampling DFT/LSR, calibrated sinefit, and LC-DS.

TABLE II
QUALITATIVE COMPARISON OF SINE WAVE ESTIMATION METHODS.

Performance metric	Uniform DFT/LSR	Calibrated sinefit [25]	LC-DS (This work)
Accuracy for large signals	Good[1]	Excellent	Good
Accuracy for small signals	Low[1]	Excellent	Excellent[2]
Computation speed for large sample size	Fast	Very slow[3]	Very fast[4]
Handles signal saturation	No	Yes	Yes

[1] Error is dominated by systematic, correlated quantization noise and does not decrease as N increases.
[2] Accuracy approaches that of the calibrated sinefit method for small-amplitude signals.
[3] Calibrated sinefit does not have a closed-form solution and relies on iterative optimization.
[4] Computation is significantly faster as it depends on the number of level crossings, not the total number of samples N.

context of fast and accurate sine wave estimation. The analysis demonstrates that LC-DS offers significant advantages over traditional methods, particularly in terms of computational efficiency and reduced quantization error. By leveraging the inherent properties of level-crossing sampling, high-resolution estimates can be achieved with reduced data sets from reference-based ADC data, making it a viable option for both real-time and low-cost applications.

The comparative study between LC-DS, uniform DFT/LSR, and the state-of-the-art calibrated sinefit method highlights the potential of LC-DS to significantly improve performance in scenarios where speed and precision are critical. For small signals, the performance of LC-DS is nearly identical to the calibrated sinefit method, and both methods are able to handle saturated signals. Furthermore, the results indicate that LC-DS can be effectively integrated into existing LSR-based systems with only small modifications to the digital signal processing block. Additionally, by looking at data reduction percentages, one can algorithmically determine the suitability of LC-DS and opt not to use the downsampled data in cases where the original data would be superior (noisy data or small data sets.) The broad EIS-based testing covered a wide bandwidth and dynamic range, therefore the results can be extrapolated to other applications that require high precision single sine wave estimation.

This paper contributes to the advancement of efficient techniques to improve the accuracy and speed of sine wave estimation, and the promising results presented in this paper pave the way for further research and development. For example, the performance of the LC-DS algorithm will be explored in more demanding conditions such as the presence of harmonics.

While this work is already integrated into a low-cost impedance analyzer [14, 15] for use in real-world environmental monitoring and diagnostic applications, future work will include custom hardware or CMOS-level implementation for the algorithm to further the goal of fast and accurate low-cost impedance analysis.

ACKNOWLEDGMENT

This work is based on the research supported by the South African Department of Science, Technology and Innovation (DSTI) Nano-Micro Manufacturing Facility (NMMF). Any opinion, finding and conclusion, or recommendation expressed in this material is that of the authors, and the funding sources do not accept any liability in this regard.

REFERENCES

[1] S. Han, Y. Yang, X. Zhao, and X. Zhang, "3D measurement method based on gray code and single sine fringe image," *Measurement*, vol. 242, p. 116182, Jan. 2025. doi: 10.1016/j.measurement.2024.116182 .

[2] E. Zendejas-Hernández, G. Trujillo-Schiaffino, M. Anguiano-Morales, D. P. Salas-Peimbert, L. F. Corral-Martínez, P. G. Mendoza-Villegas, and N. Tornero-Martínez, "Sinusoidal parameter estimation technique for three-dimensional object reconstruction

from a single object capture," *Optics Continuum*, vol. 3, no. 6, p. 962, Jun. 2024. doi: 10.1364/optcon.506198.

[3] Y. Zhuang and D. Chen, *Accurate and Robust Spectral Testing with Relaxed Instrumentation Requirements*, 1st ed. Cham: Springer International Publishing, 2018. doi: 10.1007/978-3-319-77718-4.

[4] "IEEE standard for terminology and test methods for analog-to-digital converters," 2023. doi: 10.1109/ieeestd.2023.10269815.

[5] X. Rui, P. Guo, H. Chen, S. Chen, and Y. Zhang, "Adaptive iteratively reweighted sine wave fitting method for rapid wind vector estimation of pulsed coherent doppler lidar," *Optics Express*, vol. 27, no. 15, p. 21319, Jul. 2019. doi: 10.1364/oe.27.021319.

[6] T.-S. Nguyen, T.-N. Nguyen, Q.-S. Tran, and T.-H. Huynh, "Improvement of ultrasound-based localization system using sine wave detector and CAN network," *Journal of Sensor and Actuator Networks*, vol. 6, no. 3, p. 12, Jul. 2017. doi: 10.3390/jsan6030012.

[7] L. Zhang, Y. Liu, R. Wang, P. Allen, L. Lyu, and J. Feng, "Advanced vibration control strategies for electro-hydraulic testing systems focus on sinusoidal swept-frequency techniques," *Measurement*, vol. 246, p. 116711, Mar. 2025. doi: 10.1016/j.measurement.2025.116711.

[8] J. Zhang, J. Song, C. Li, X. Xu, and H. Wen, "Novel frequency estimator for distorted power system signals using two-point iterative windowed DFT," *IEEE Transactions on Industrial Electronics*, vol. 71, no. 10, pp. 13 372–13 383, Oct. 2024. doi: 10.1109/tie.2023.3347846.

[9] R. M. Bruce, P. A. Phan, E. Pacpaco, N. M. Rahman, and A. D. Farmery, "The inspired sine-wave technique: A novel method to measure lung volume and ventilatory heterogeneity," *Experimental Physiology*, vol. 103, no. 5, pp. 738–747, May 2018. doi: 10.1113/ep086867.

[10] T. Arts, F. W. Prinzen, T. Delhaas, J. R. Milles, A. C. Rossi, and P. Clarysse, "Mapping displacement and deformation of the heart with local sine-wave modeling," *IEEE Transactions on Medical Imaging*, vol. 29, no. 5, pp. 1114–1123, May 2010. doi: 10.1109/tmi.2009.2037955.

[11] Q. Song, J. Liu, and Y. Liu, "Novel low-speed measuring method based on sine and square wave signals," *Metrology*, vol. 3, no. 1, pp. 82–98, Feb. 2023. doi: 10.3390/metrology3010005.

[12] S. Lin, C. Rothleitner, N. Rogge, and T. Fröhlich, "Influences on amplitude estimation using three-parameter sine fitting algorithm in the velocity mode of the planck-balance," *Acta Imeko*, vol. 9, no. 3, p. 40, Sep. 2020. doi: 10.21014/acta_imeko.v9i3.781.

[13] A. De Angelis, F. Santoni, A. Moschitta, and P. Carbone, "Design and implementation of a low cost system for accurate impedance spectroscopy," in *2022 IEEE International Symposium on Systems Engineering (ISSE)*. Vienna, Austria: IEEE, Oct. 2022, pp. 1–6. doi: 10.1109/isse54508.2022.10005507.

[14] D. J. De Beer and T.-H. Joubert, "Undersampling and saturation for impedance spectroscopy performance," *IEEE Sensors Journal*, vol. 21, no. 20, pp. 23 382–23 389, Oct. 2021. doi: 10.1109/jsen.2021.3105317.

[15] ——, "Validation of low-cost impedance analyzer via nitrate detection," *Sensors*, vol. 21, no. 19, p. 6695, Oct. 2021. doi: 10.3390/s21196695.

[16] V. Viswam, R. Bounik, A. Shadmani, J. Dragas, C. Urwyler, J. A. Boos, M. E. J. Obien, J. Muller, Y. Chen, and A. Hierlemann, "Impedance spectroscopy and electrophysiological imaging of cells with a high-density CMOS microelectrode array system," *IEEE Transactions on Biomedical Circuits and Systems*, vol. 12, no. 6, pp. 1356–1368, Dec. 2018. doi: 10.1109/tbcas.2018.2881044.

[17] D. W. Scott and Y. Alseiha, "Determining detection limits of aqueous anions using electrochemical impedance spectroscopy," *Journal of Analytical Science and Technology*, vol. 8, no. 1, pp. 1–5, Dec. 2017. doi: 10.1186/s40543-017-0126-9.

[18] A. V. Oppenheim and R. W. Schafer, Eds., *Discrete-Time Signal Processing*, 3rd ed., ser. Prentice Hall Signal Processing Series. Upper Saddle River Munich: Pearson, 2010.

[19] M. J. Pelgrom, *Analog-to-Digital Conversion*. Cham: Springer International Publishing, 2022. doi: 10.1007/978-3-030-90808-9.

[20] F. C. Alegria, "Bias of amplitude estimation using three-parameter sine fitting in the presence of additive noise," *Measurement*, vol. 42, no. 5, pp. 748–756, Jun. 2009. doi: 10.1016/j.measurement.2008.12.006.

[21] D. Bellan, "On the validity of the noise model of quantization for the frequency-domain amplitude estimation of low-level sine waves," *Metrology and Measurement Systems*, vol. 22, no. 1, pp. 89–100, Mar. 2015. doi: 10.1515/mms-2015-0004.

[22] P. Carbone and J. Schoukens, "A rigorous analysis of least squares sine fitting using quantized data: The random phase case," *IEEE Transactions on Instrumentation and Measurement*, vol. 63, no. 3, pp. 512–530, Mar. 2014. doi: 10.1109/tim.2013.2282220.

[23] D. Belega, D. Dallet, and D. Petri, "Performance comparison of the three-parameter and the four-parameter sine-fit algorithms," in *2011 IEEE International Instrumentation and Measurement Technology Conference*. Hangzhou, China: IEEE, May 2011, pp. 1–4. doi: 10.1109/imtc.2011.5944010.

[24] Z. Liang, D. Ren, J. Sun, and Z. Zhu, "Fitting algorithm of sine wave with partial period waveforms and non-uniform sampling based on least-square method," *Journal of Physics: Conference Series*, vol. 1149, no. 1, p. 12019, Dec. 2018. doi: 10.1088/1742-6596/1149/1/012019.

[25] P. Carbone, B. Renczes, A. De Angelis, and A. Moschitta, "Calibrated sinefit based on quantized data," in *2024 IEEE International Instrumentation and Measurement Technology Conference (I2MTC)*. Glasgow, United Kingdom: IEEE, May 2024, pp. 1–6. doi: 10.1109/I2MTC60896.2024.10560811.

[26] B. Renczes, A. De Angelis, A. Moschitta, and P. Car-

bone, "Sinewave fitting based on quantization codes and threshold levels," *IEEE Transactions on Instrumentation and Measurement*, vol. 74, pp. 1–11, 2025. doi: 10.1109/TIM.2025.3544373 .

[27] F. Harris, "On the use of windows for harmonic analysis with the discrete fourier transform," *Proceedings of the IEEE*, vol. 66, no. 1, pp. 51–83, 1978. doi: 10.1109/proc.1978.10837 .

[28] Jian Qiu Zhang, Zhao Xinmin, Hu Xiao, and Sun Jinwei, "Sinewave fit algorithm based on total least-squares method with application to ADC effective bits measurement," *IEEE Transactions on Instrumentation and Measurement*, vol. 46, no. 4, pp. 1026–1030, 1997. doi: 10.1109/19.650821 .

[29] P. Handel, "Parameter estimation employing a dual-channel sine-wave model under a gaussian assumption," *IEEE Transactions on Instrumentation and Measurement*, vol. 57, no. 8, pp. 1661–1669, Aug. 2008. doi: 10.1109/tim.2008.923782 .

[30] A. Zanjani and M. Jalali, "A power-efficient level-crossing analog-to-digital converter with adaptive resolution based on a signal-dependent sampling mechanism," *Circuits, Systems, and Signal Processing*, vol. 42, no. 1, pp. 63–83, Jan. 2023. doi: 10.1007/s00034-022-02146-9 .

[31] J. Stewart, D. Clegg, and S. Watson, *Calculus: Early Transcendentals*, 9th ed. Boston, MA: Cengage, 2021.

D. Johan De Beer (Member, IEEE) received the B.Eng and B.Eng (Hons.) degrees in electronic engineering with distinction from the University of Pretoria, South Africa, and had his M.Eng degree upgraded to a Ph.D. level which has been submitted for examination at the Department of Electrical, Electronic and Computer Engineering. He is currently researching emerging sensor technologies for the Carl and Emily Fuchs Institute for Microelectronics (CEFIM). His research interests include emerging sensor technologies, low-cost design methodologies, and mixed-signal CMOS design. He has gained valuable experience as a Visiting Student Researcher at Colorado State University, working with the Henry Group in Chemical Research under a Fulbright Scholarship. His work included researching novel sensing technologies using electrochemical instrumentation and collaborating on the design of an electrochemical, label-free method for detecting heart failure biomarkers in blood. His current research at the University of Pretoria focuses on developing a low-cost impedance analyzer using CMOS technology. This device aims to measure the impedance of various electronic components and materials, which is crucial for applications in biomedical engineering, material science, and electronics.

Trudi-H. Joubert (Senior Member, IEEE) is the Director of the Carl and Emily Fuchs Institute for Microelectronics (CEFIM) at the University of Pretoria, as well as the Director of the Printed Electronics node of the Nano-Micro Manufacturing Facility. She is registered as a professional engineer with the Engineering Council of South Africa (ECSA). She received both the B.Eng and M.Eng degrees in electronic engineering with distinction, and earned a Ph.D in electronic engineering from the University of Pretoria, South Africa. Her core pursuit is CMOS and BiCMOS mixed signal circuit design, mainly in readout and signal processing for imaging arrays, biologically inspired electronic circuit applications, and specialised devices for analog IC design. Her most recent endeavour is integrated printed electronics circuits for point-of-need physical, electrochemical, and optical sensor microsystems. She is a C2 NRF-rated researcher who has been awarded more than R 41 million research grant funding. She is the inventor of three patents, and has published 31 journal papers, presented and co-authored 66 peer-reviewed conference proceedings papers. She has been a member of both the technical and the organising committee for several international conference events, and acts as reviewer for high impact factor journals. She supervised several graduate students, while also acting as external examiner for other institutions. She has lectured 10 short courses to industry in her field of specialization, worked on 31 projects for the South African industry, writing 139 technical reports in the process, and contributing to 32 integrated circuit chips. The contributions of her work to the South African innovation system spans university teaching, applied research, and leading industrial development of prototypes and products.